Boundary-Locality and Perturbative Structure of Entanglement Spectra in Gapped Systems

Vincenzo Alba,[1] Masudul Haque,[1] and Andreas M. Läuchli[1,2]

[1]*Max-Planck-Institut für Physik komplexer Systeme, Nöthnitzer Straße 38, D-01187 Dresden, Germany*

[2]*Institute für Theoretische Physik, Universität Innsbruck, A-6020 Innsbruck, Austria*

(Received 15 July 2011; published 29 May 2012)

The entanglement between two parts of a many-body system can be characterized in detail by the entanglement spectrum. Focusing on gapped phases of several one-dimensional systems, we show how this spectrum is dominated by contributions from the boundary between the parts. This contradicts the view of an ''entanglement Hamiltonian'' as a bulk entity. The boundary-local nature of the entanglement spectrum is clarified through its hierarchical level structure, through the combination of two single-boundary spectra to form a two-boundary spectrum, and finally through consideration of dominant eigenfunctions of the entanglement Hamiltonian. We show consequences of boundary-locality for perturbative calculations of the entanglement spectrum.

DOI: 10.1103/PhysRevLett.108.227201 PACS numbers: 75.10.Pq, 03.67.−a, 05.30.−d

Introduction.—The study of entanglement-related quantities in condensed matter has led to a large body of interdisciplinary work [1]. Recently, the concept of the entanglement spectrum has established itself at the forefront of the field, as this spectrum provides much finer information than a single number like the von Neumann entropy. Considering a bipartition of the system into parts A and B, the entanglement spectrum (ES), $\{\xi_i\}$, is defined in terms of the Schmidt decomposition

$$|\psi\rangle = \sum_i e^{-\xi_i/2} |\psi_i^A\rangle \otimes |\psi_i^B\rangle. \quad (1)$$

Here, $|\psi\rangle$ is the ground state, and the states $|\psi_i^A\rangle$ ($|\psi_i^B\rangle$) form an orthonormal basis for the subsystem A (B). The ES $\{\xi_i = -\log\lambda_i\}$ can also be thought of in terms of the eigenvalues $\{\lambda_i\}$ of the reduced density matrix ρ_A obtained after tracing out the B part of the system density matrix $|\psi\rangle\langle\psi|$.

The ES has been studied earlier for insights into the density matrix renormalization group (DMRG) algorithm [2–4] and more recently because of its relation to low-energy boundary-related modes in topological phases [5–7]. One way of thinking of the ES is in terms of an entanglement Hamiltonian (EH) $H_A = -\log\rho_A$ acting only on the A degrees of freedom [3,9–12]. The ES is then the spectrum of this object. This gives a suggestive correspondence to the energy spectrum of true bulk Hamiltonians. This idea has also inspired calculations of bulk terms that appear in such a ''Hamiltonian'' [3,9]. In topologically ordered systems such as fractional quantum Hall states, the EH indeed seems to share the low-lying edge modes with the physical Hamiltonian of a system with the same boundary. This correspondence gave rise to the loose idea that entanglement Hamiltonians are quite similar to physical ''bulk'' Hamiltonians, apart perhaps from nonessential renormalizations, such as longer range hoppings or spatial inhomogeneities [5,6]. However, the well-known area law for the entanglement entropy $S_A = -\sum \lambda_i \log\lambda_i$, stating that S_A scales with the size of the boundary between A and B parts, clearly suggests that the spectrum of ρ_A (and hence also the ES and EH) must in some sense be dominated by the boundary degrees of freedom.

This contradiction is highlighted even more by considering states that are described by simple matrix product states, such as the Majumdar-Ghosh point in the frustrated antiferromagnetic chain (J_1-J_2 model) or the AKLT (Affleck-Kennedy-Lieb-Tasaki) state [13]. The entanglement spectrum for these states consists only of a small number of finite values, independent of the (sufficiently large) block size A. These simple gapped states thus clearly have entanglement spectra determined completely by the boundary and not by the bulk.

In this Letter, we sharpen the boundary picture of the entanglement spectrum by considering more general gapped one-dimensional (1D) systems. The boundary-local nature of the ES is demonstrated and made quantitative in several ways. We show that the ES of gapped states generally have a hierarchical structure, with excitations farther from the boundary being successively higher in the ES. This also leads us to the idea that the ES can be obtained from a boundary-connected perturbative calculation, and we show elements of such a calculation. We also show that the ES of two-boundary blocks can be constructed by combining the ES of single-boundary blocks, demonstrating that the bulk degrees of freedom play a secondary role. We will concentrate on the widely familiar XXZ chain, and as a bonus, we uncover a beautiful set of degeneracy structures in the ES of this model. We believe these findings are very general; we emphasize this by briefly presenting boundary-locality in two other systems, namely, the Heisenberg ladder and the Mott insulating phase of the Bose-Hubbard model.

In our examples we consider perturbations around a product state; it should be possible to adapt to perturbations

around a point which is a matrix product state with small-rank matrices. Gapped 1D phases often contain or are connected to such simple points. Gapped phases in general are not very universal in their low-energy properties; it is therefore remarkable that the ES has features common in many gapped phases, which we identify in this work.

The usual methods for calculating ES are numerical exact diagonalization or DMRG, or using two-point correlators for noninteracting systems [2]. We propose our boundary-linked perturbation theory as a general alternate technique for calculating ES in gapped phases containing a simple point around which one can perturb. The basic insight is that, while calculating the complete reduced density matrix perturbatively requires perturbation terms acting on the whole system or block, if one is only interested in determining the ES and the leading order eigenfunctions (entanglement eigenstates), then a boundary-local perturbation theory is able to construct the ES order by order in a physically transparent way.

Boundary-linked perturbation theory.—To obtain ES levels correctly up to nth order, one only needs to consider perturbations up to this order which act within αn sites from the boundary, α depending on the type of perturbation. This is a direct but powerful consequence of boundary-locality, namely, that the ES levels at increasing orders correspond to increasing distances from the boundary. The perturbative calculation necessary for calculating ES levels is thus ''boundary-linked''.

For any two orthonormal bases $|\varphi_i^A\rangle$, $|\varphi_j^B\rangle$, of subsystems A and B, the system wave function can be written as $|\psi\rangle = \sum_{i,j} \mathbf{M}_{ij} |\varphi_i^A\rangle \otimes |\varphi_j^B\rangle$. The $e^{-\xi_i/2}$ of Eq. (1) are obtained from a singular value decomposition (SVD) of the matrix $\mathbf{M}$. Further aspects of the perturbative calculation of ES can be formulated in terms of the matrix $\mathbf{M}$. For example, when calculating $\mathbf{M}$ perturbatively, we find that a contribution to $\mathbf{M}$ at some order can lead to a new ES level only if the contribution is not appearing on the same row or the same column as a previous contribution which led to a new ES level at lower order. In physical terms, this means that we do not get new ES levels by applying a perturbation only to the A block but need to apply perturbation terms to both blocks in a linked way. Some perturbative calculations for the Heisenberg spin ladder, and some general perturbative features of the matrix $\mathbf{M}$, appear in the Supplemental Material [14].

The XXZ gapped phase.—We consider the anisotropic Heisenberg (XXZ) chain, $\mathcal{H} \equiv \mathcal{H}_z + \mathcal{H}_{xy}$, with $\mathcal{H}_z \equiv \Delta \sum_i S_i^z S_{i+1}^z$, and $\mathcal{H}_{xy} \equiv \frac{1}{2} \sum_i (S_i^+ S_{i+1}^- + \text{H.c.})$, in the gapped phase $\Delta > 1$. The Ising limit $\Delta \gg 1$ is simple: the ground state is spanned by the two product (Néel) states $|N1\rangle \equiv |\uparrow\downarrow\uparrow\downarrow\uparrow\downarrow \cdots\rangle$ and $|N2\rangle \equiv |\downarrow\uparrow\downarrow\uparrow\downarrow\uparrow \cdots\rangle$. We will therefore think perturbatively around this simple limit, $\mathcal{H}_{xy}$ being the perturbation. In the language of ''domain walls'' (bond between neighboring aligned spins), the perturbation $\mathcal{H}_{xy}$ can have two effects: it can create a pair of domain walls situated two bonds apart or it can move a domain wall over two sites. We choose for simplicity to work with perturbations around a single Néel state, by selecting $|N1\rangle$ instead of the linear combination $\frac{1}{\sqrt{2}}(|N1\rangle + |N2\rangle)$ to be the vacuum state. For cases where the linear combination is appropriate, the ES can readily be reconstructed from knowledge about the individual Néel states by overlaying and shifting by log 2 of the single-state ES.

The XXZ single-boundary ES.—Figure 1(a) shows the ES for the simplest setup, namely, a single boundary partitioning an open XXZ chain into two long blocks. The total S^z of the block A is a good quantum number for the reduced density matrix ρ_A. Hence, we organize the ES into sectors of δS_A^z, which is the difference of the S_A^z value of the corresponding entanglement eigenstate from the block S^z value in the Néel state (0 or $\pm\frac{1}{2}$). The most notable feature is that the ES is organized in equally spaced hierarchical levels. In Figs. 1(a) and 1(e) the hierarchical orders are denoted as ''perturbation order'' because successive orders in a perturbative calculation yield successively higher ES levels.

Higher levels correspond to excitations farther from the boundary. In Figs. 1(c) and 1(d) this is illustrated pictorially by showing the dominant configurations in some of the states occurring at several levels.

The ES can be understood physically, and constructed accurately and completely, through the boundary-linked perturbation theory introduced previously. Here, we present a qualitative discussion highlighting the algebraic structure of the problem. For the XXZ model, this theory can be formulated as follows. The vacuum state has no domain walls. Excitations in the ES are obtained by introducing domain walls near the boundary and by moving them into the bulk. From explicit perturbative calculations at the first few orders, we find that the only perturbation terms leading to new ES levels are those which do one of the following: (1) create a pair of domain walls by applying $\mathcal{H}_{xy}$ across the boundary,

$$\ldots \sigma\sigma\, \uparrow\downarrow][\uparrow\downarrow\, \sigma\sigma \ldots \rightsquigarrow \ldots \sigma\sigma \underline{\uparrow\uparrow}][\underline{\downarrow\downarrow} \sigma\sigma \ldots, \qquad (2)$$

or (2) act twice, on the first bonds on either side of the boundary, again creating a domain wall pair

$$\ldots \sigma\, \downarrow\uparrow][\uparrow\downarrow\uparrow\, \sigma \ldots \rightsquigarrow \ldots \sigma \underline{\downarrow\downarrow}\, \uparrow][\downarrow \underline{\uparrow\uparrow} \sigma \ldots, \qquad (3)$$

or (3) act twice symmetrically with respect to the boundary so as to move a domain wall on each block, each by two bonds away from the boundary. Above, domain wall positions are shown underlined, and σ represents a spin of unspecified orientation. The first process changes S_A^z by ± 1, while the others preserve S_A^z. The boundary-locality of the ES is encoded in the restriction that domain walls are created only through the first two processes above and not farther away from the boundary. The symmetrical pairwise

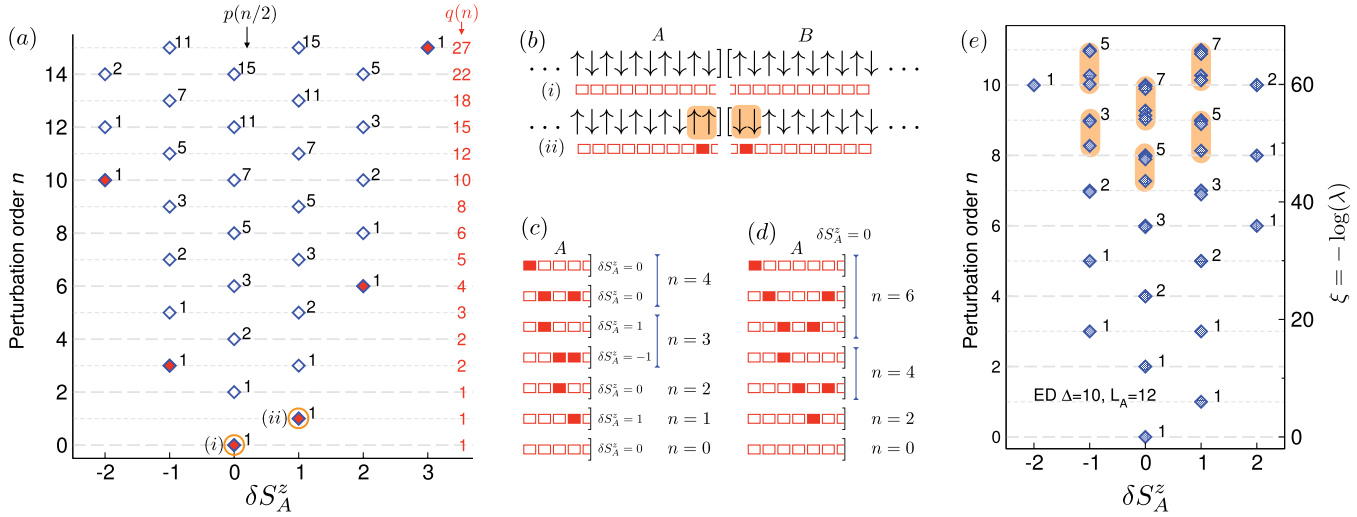

FIG. 1 (color online). Single boundary ES of the XXZ chain. (a) Long or infinite blocks. The ES levels appear at well-defined levels, which correspond to successive perturbative orders n. The accompanying integers denote degeneracies. On the right we show the total degeneracies at each order. The levels marked (i) and (ii) have dominant contributions shown in (b), where a filled-rectangle notation is introduced for domain walls. (c) Dominant contributions to low-lying levels. (d) Dominant contributions to low-lying $\delta S^z_A = 0$ levels. (e) Finite-size block (12 spins in A); arbitrary-precision exact diagonalization data for $\Delta = 10$. The effects of finite size are seen through breaking of degeneracies at order ~ 8 and higher. The integer-indicated degeneracies are now approximate.

application of $\mathcal{H}_{xy}$ ensures that the new contribution is to an element of the $\mathbf{M}$ matrix that is not on the same row or column as a previous element that already led to a lower order ES level.

Given a domain wall configuration, the corresponding A state belongs to the sector $\delta S^z_A = (-1)^{N_D} \frac{1}{2} \sum_j (-1)^j \times [1 - (-1)^{\ell_j}]$, where N_D is the number of domain walls in A, $j \in [1, N_D]$ labels those starting from the boundary, and $\ell_j \geq 1$ is the position of the jth domain wall measured from the cut. In our perturbative rules, the order at which a particular configuration appears is given by $n = \sum_j \ell_j$. One can thus construct the ES, organized by δS^z_A sector, from the perturbative rules in terms of the domain walls. In this way, one obtains exactly the ES of Fig. 1(a).

For each δS^z_A, the lowest ES level [filled symbols in Fig. 1(a)] is generated by a state where the region near the boundary is packed with domain walls at each bond, creating a ferromagnetic region as large as needed to have that δS^z_A value. The lowest level for sector δS^z_A occurs at order $m(\delta S^z_A) = |\delta S^z_A (2\delta S^z_A - 1)|$.

The degeneracies of the ES follow intriguing patterns, which can be explained through our construction. The degeneracy at order n in a given δS^z_A tower is $p([n - m(\delta S^z_A)]/2)$ where $p(x)$ is the number of integer partitions of the integer x. The total degeneracy at a given order n, listed to the right of Fig. 1(a), is given by $q(n)$, the number of partitions into unequal summands [15]. The degeneracy sequence $q(n)$ was observed in corner transfer matrix calculations [16], but our perturbative construction now gives a physical picture: the number of ES levels at order n is the number of ways one can place domain walls within the first n positions while keeping the sum of position labels ($\sum_j \ell_j$) to be n; this number is $q(n)$ by definition.

For the infinite XXZ chain, this ES is actually exact for all $\Delta > 1$ (not just $\Delta \gg 1$), with the ES level spacing $2\,\mathrm{arccosh}\Delta$, as a result of integrability [16]. In a generic (nonintegrable) gapped phase, the hierarchical level structure is most pronounced in the case of weak perturbations and gets progressively broadened by higher order renormalizations of entanglement levels upon increasing the perturbation.

Figure 1(e) plots the exact ES for a finite open chain. The ES follows the infinite-system structure at low orders and only deviates significantly (e.g., split degeneracies) at orders corresponding to the distance between the boundary and the physical edge. This illustrates again that the lowest ES levels correspond to smallest distances from the partition boundary.

The two-boundary ES.—Boundary-locality implies that the single-boundary ES is sufficient to construct the ES for multiple-boundary blocks when the boundaries are sufficiently far apart. Formally, this physical intuition means that the reduced density matrix ρ_A of a two-boundary block should "factorize" in the loose sense that ρ_A is isospectral to $\rho_L \otimes \rho_R$, where $\rho_{L(R)}$ are (virtual) reduced density matrices appropriate for single-boundary blocks having the left (right) boundary of A. This idea has recently be shown to be at work for ES of blocks of a fractional quantum Hall state on the torus [6].

Figure 2 shows the combination of two single-boundary ES to form a two-boundary ES in an XXZ chain. The case

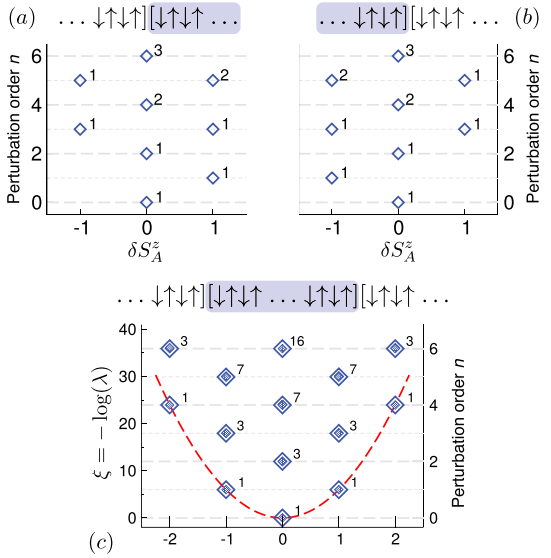

FIG. 2 (color online). Combining two single-boundary ES to form a two-boundary ES, for the XXZ chain. Shading indicates the A partition. (a and b) The single-boundary ES obtained by considering two different bipartitions. (c) Combination of single-boundary cases to form a two-boundary ES (large empty diamonds), compared with numerical diagonalization data at $\Delta = 10$ (small filled diamonds), which match perfectly.

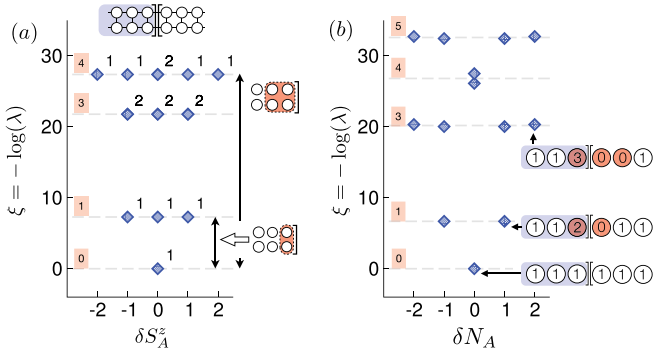

FIG. 3 (color online). Single-boundary ES (DMRG data) for the (a) Heisenberg spin ladder and (b) Bose–Hubbard chain. For the ladder, we show numerical data for $J_{\rm leg} = 0.1 J_{\rm rung}$, in the rung singlet phase. The partitioning is shown in the top cartoon (region A shaded as in Fig. 2). The integers next to the data points indicate approximate degeneracies. In the associated cartoons, we show with shading the rungs (degrees of freedom) which contribute to various levels of the ES. For the Bose–Hubbard case (data shown for $U = 40$), the cartoons show dominant contributions to ES levels. Sites with occupancy $\neq 1$ are shaded; occupancies are indicated with integers on each site. Partition A is again as in Fig. 2. In both panels the horizontal light dashed lines are guides to the eye indicating the perturbation order at which the levels appear.

shown corresponds to the ground state being a dressed single Néel state $|N1\rangle$, and an even size for the A block. The relevant single-edge ES, Figs. 2(a) and 2(b), are then (δS^z_A)-inverted versions of each other. Each level of Fig. 2(a) is combined with each level of Fig. 2(b), the two constituents contributing additively to the order and to δS^z_A. The resulting ES has the structure and degeneracies shown in Fig. 2(c). In the combined ES, the lowest level at any δS^z_A is found, from a combination of $m_L(x) = |x(2x+1)|$ and $m_R(x) = |x(2x-1)|$, to be $m(\delta S^z_A) = (\delta S^z_A)^2$. This explains the parabolic envelope shown as a dashed line in Fig. 2(c).

If the A block is odd instead of even, the two single-boundary ES are identical rather than reflections of each other; the combined ES would then not be symmetric under δS^z_A inversion.

Other gapped 1D systems.—Boundary-locality can be illustrated with the ES of various other gapped systems. As a first additional example, we demonstrate in Fig. 3(a) the case of the gapped spin-$\frac{1}{2}$ Heisenberg ladder [17] with a cut which bisects both chains (in contrast to the chain-chain setup studied in Refs. [10,12,18]). There is once again a hierarchical level structure corresponding to increasing distances from the boundary. The levels have $SU(2)$ structure; there is a triplet at first order, no new levels at second order, two triplets at third order, a singlet and a quintuplet at fourth order, etc. Boundary-linked perturbation arguments can explain this structure and also the parabolic envelope.

Our last example system is the Bose–Hubbard chain in the gapped Mott insulating phase at unit filling [Fig. 3(b)]. The level structures in the ES are richer than the XXZ or ladder cases, due to the larger local Hilbert space. Some features, like a near-parabolic envelope, appeared in Ref. [19]. Here, we provide the physical picture behind this observation based on boundary-locality, as illustrated through the cartoons in Fig. 3. The nature of the local Hilbert spaces now allow asymmetric excitations in the two blocks, leading to a modified parabola for the envelope: $\xi \approx x(x+1)\ln U - \ln[(x+1)!] + \mathcal{O}(1/U)$, with $x = |\delta N_A|$.

Conclusions.—While entanglement as a boundary-related quantity is a direct reflection of the area law and is thus well-appreciated, the competing picture of a bulk entanglement Hamiltonian clearly calls for a thorough exploration of boundary-locality and its consequences. We have provided the elements of such an analysis here. In particular, we have shown how boundary-locality allows a perturbative formalism specific to calculating entanglement spectra. At any finite perturbative order, we reproduce a finite number of the lowest ES levels, which amounts to constructing a finite-rank matrix product representation of the state.

To put our work in the context of recent literature, high-temperature series expansions for the mutual information exhibit a boundary-linked property [20] similar to our rather different $T = 0$ perturbation theory targeting ES. Other recent works highlighted the structure of ES along a 1D

block boundary in 2D systems [18,8]. Our work is complementary in that we clarify the structure of the ES perpendicular to the cut, i.e., as one moves further into the bulk.

Our work opens up several research avenues. For example, in gapless 1D states and in Fermi liquids in higher dimensions, the entanglement entropy does not scale purely with the boundary size but has a logarithmic correction. This implies some kind of weakening of the boundary-local picture; degrees of freedom deep in the bulk must play a greater role in such cases. Quantifying this effect remains an open task.

[1] L. Amico *et al.*, Rev. Mod. Phys. **80**, 517 (2008).

[2] M.-C. Chung and I. Peschel, Phys. Rev. B **64**, 064412 (2001).

[3] I. Peschel and V. Eisler, J. Phys. A **42**, 504003 (2009).

[4] K. Okunishi, Y. Hieida, and Y. Akutsu, Phys. Rev. E **59**, R6227 (1999).

[5] H. Li and F. D. M. Haldane, Phys. Rev. Lett. **101**, 010504 (2008).

[6] A. M. Läuchli, E. J. Bergholtz, J. Suorsa, and M. Haque, Phys. Rev. Lett. **104**, 156404 (2010).

[7] R. Thomale, D. P. Arovas, and B. A. Bernevig, Phys. Rev. Lett. **105**, 116805 (2010); Z. Papic, B. A. Bernevig, and N. Regnault, Phys. Rev. Lett. **106**, 056801 (2011); N. Regnault, B. A. Bernevig, and F. D. M. Haldane, Phys. Rev. Lett. **103**, 016801 (2009); F. Pollmann *et al.*, Phys. Rev. B **81**, 064439 (2010); N. Bray-Ali, L. Ding, and S. Haas, Phys. Rev. B **80**, 180504(R) (2009); A. M. Turner, Y. Zhang, and A. Vishwanath, Phys. Rev. B **82**, 241102R (2010); A. M. Turner *et al.*, Phys. Rev. B **85**, 165120 (2012); M. Kargarian and G. Fiete, Phys. Rev. B **82**, 085106 (2010); E. Prodan, T. L. Hughes, and B. A. Bernevig, Phys. Rev. Lett. **105**, 115501 (2010); T. L. Hughes, Phys. Rev. B **83**, 245132 (2011); L. Fidkowski, Phys. Rev. Lett. **104**, 130502 (2010); L. Fidkowski, T. S. Jackson, and I. Klich, Phys. Rev. Lett. **107**, 036601 (2011).

[8] X. Qi, H. Katsura, and A. W. W. Ludwig, Phys. Rev. Lett. **108**, 196402 (2012).

[9] B. Nienhuis, M. Campostrini, and P. Calabrese, J. Stat. Mech. (2009) P02063.

[10] D. Poilblanc, Phys. Rev. Lett. **105**, 077202 (2010).

[11] J. Schliemann, Phys. Rev. B **83**, 115322 (2011).

[12] I. Peschel and M.-C. Chung, Europhys. Lett. **96**, 50006 (2011); A. M. Läuchli and J. Schliemann, Phys. Rev. B **85**, 054403 (2012).

[13] D. Pérez-García *et al.*, Quantum Inf. Comput. **7**, 401 (2007).

[14] See Supplemental Material at http://link.aps.org/supplemental/10.1103/PhysRevLett.108.227201 for details of the perturbative ES structure in the Heisenberg spin ladder and for a general proof of boundary locality at low perturbation orders, in generic gapped 1D systems.

[15] The functions $p(n)$ and $q(n)$ generate sequences A000041 and A000009 in the Online Encyclopedia of Integer Sequences, http://oeis.orghttp://oeis.org.

[16] I. Peschel, M. Kaulke, and O. Legeza, Ann. Phys. **8**, 153 (1999).

[17] E. Dagotto and T. M. Rice, Science **271**, 618 (1996).

[18] J. I. Cirac, D. Poilblanc, N. Schuch, and F. Verstraete, Phys. Rev. B **83**, 245134 (2011).

[19] X. Deng and L. Santos, Phys. Rev. B **84**, 085138 (2011).

[20] R. R. P. Singh, M. B. Hastings, A. B. Kallin, and R. G. Melko, Phys. Rev. Lett. **106**, 135701 (2011).